RESEARCH ARTICLE

Dynamic downscaling of near-surface air temperature at the basin scale using WRF—a case study in the Heihe River Basin, China

Xiaoduo PAN (✉), Xin Li, Xiaokang SHI, Xujun HAN, Lihui LUO, Liangxu WANG

Cold and Arid Regions Environmental and Engineering Research Institute, Chinese Academy of Sciences, Lanzhou 730000, China

Abstract The spatial resolution of general circulation models (GCMs) is too coarse to represent regional climate variations at the regional, basin, and local scales required for many environmental modeling and impact assessments. Weather research and forecasting model (WRF) is a next-generation, fully compressible, Euler non-hydrostatic mesoscale forecast model with a run-time hydrostatic option. This model is useful for downscaling weather and climate at the scales from one kilometer to thousands of kilometers, and is useful for deriving meteorological parameters required for hydrological simulation too. The objective of this paper is to validate WRF simulating 5 km/ 1 h air temperatures by daily observed data of China Meteorological Administration (CMA) stations, and by hourly in-situ data of the Watershed Allied Telemetry Experimental Research Project. The daily validation shows that the WRF simulation has good agreement with the observed data; the R^2 between the WRF simulation and each station is more than 0.93; the absolute of meanbias error (MBE) for each station is less than 2°C; and the MBEs of Ejina, Mazongshan and Alxa stations are near zero, with R^2 is more than 0.98, which can be taken as an unbiased estimation. The hourly validation shows that the WRF simulation can capture the basic trend of observed data, the MBE of each site is approximately 2°C, the R^2 of each site is more than 0.80, with the highest at 0.95, and the computed and observed surface air temperature series show a significantly similar trend.

Keywords weather research and forecasting model, dynamic downscaling, surface air temperature, Heihe River Basin, Watershed Allied Telemetry Experimental Research Project

1 Introduction

The spatial resolution of general circulation models (GCMs) is too coarse to represent regional, basin, and local climate variations at the scales required for many environmental modeling and impact assessments. Two techniques have been developed that counter this deficiency: semi-empirical (statistical) downscaling (SDS) of GCM outputs and dynamic downscaling using regional climate models (RCMs) nested within a GCM. A key strength of SDS is the low computational demand, which facilitates the generation of ensembles of climate realizations (Wilby et al., 2000). However, realistic SDS scenarios are contingent on strong stationary empirical relationships and on the choice of predictor variable(s) and transfer function(s) used for the downscaling (Winkler et al., 1997). RCMs are computationally demanding more computer time than SDS to compute equivalent scenarios. However, with the progress of computing speed, the main advantage of RCMs (Wilby et al., 1999) is that their ability to respond in physically consistent ways to different external forcings (such as land-surface or atmospheric chemistry changes) will be greatly improved.

Leander and Buishand (2007) and Leander et al. (2008) assessed the effect of climatic change on the flood quantiles of the French-Belgian River Meuse by precipitation and temperature data from three RCMs. Lu et al. (2006) coupled Canadian mesoscale compressible community (MC2) model with Xin'anjiang hydrological model and obtained a good result of flood timing and peak discharges at the Wangjiabao Station. Collischonn et al. (2005) analyzed the flow forecasting of River Uruguay by five alternative rainfall forecasts: zero, three scales rainfall forecasting from advanced regional prediction system (ARPS) and observation trend analysis data. Kunstmann and Stadler (2005) and Kunstmann et al. (2008) coupled mesoscale model version 5 (MM5) with the distributed

hydrological model (WaSIM) for high-resolution runoff simulation in the Mangfall River catchment and for developing decision support system in the Volta Basin, respectively. Jasper et al. (2002) compared the performance of five different high-resolution numerical weather prediction models (with resolutions between 2 km×2 km and 14 km×14 km) for the prediction of peak flows in the Alpine Ticino-Toce watershed. Yu et al. (2002) linked a hydrologic model system (HMS) to a RCM, which was designed to provide fine spatio-temporal output for hydrologic and other applications, to model a series of storm events passing over the Susquehanna River Basin and to simulate various hydrologic processes in soil, land surface, and groundwater hydrology using observed and modeled storm events. Chen et al. (2006) coupled the fifth-Generation Penn State University / the National Center for Atmospheric Research (PSU/NCAR) MM5 with distributed water-heat coupled model (DWHC) to simulate runoff, the result from coupled model was much better than that driven by observation data of meteorological and hydrological stations.

It is convenient to couple RCM with land surface models. The results from this coupled model have been validated by observed land surface states; however, the validation of forcing data have been omitted, especially by high temporal resolution observed data. As Cosgrove et al. (2003) stated, "*No matter how sophisticated their depiction of land surface processes, or how accurate their boundary and initial conditions are, such models will not produce realistic results if the forcing data is not accurate.*" Thus, it is important to validate the accuracy of forcing data from RCM before they are inputted to a land surface model.

The objective of this paper is to validate weather research and forecasting model (WRF) simulating 5 km/1 h air temperatures by daily observed data from China Meteorological Administration (CMA) stations using, by hourly in-situ data from the Watershed Allied Telemetry Experimental Research (WATER) Project (for a detail introduction about WATER, Li et al., 2009), and by GCM reanalysis, respectively. The paper was organized as follows. Data and the WRF model description and configuration are introduced in Sect. 2. The long-term spatial-temporal temperature characteristic of the Heihe River Basin, daily validation, hourly validation and comparison with GCM reanalysis are described in Sect. 3. The discussion and conclusions are presented in Sects. 4 and 5, respectively.

2   Data and WRF model

2.1   WRF model and its configuration and initialization

The WRF (Michalakes et al., 1998; 2001) model is a next-generation mesoscale numerical weather prediction system that serves both operational and research communities. The WRFV3.1 system consists of multiple dynamical cores, preprocessors for producing initial and lateral boundary conditions for simulations, and a four-dimensional variational data assimilation (4DVAR) system. WRF is built by using software tools to enable extensibility and efficient computational parallelism. The use of the WRF system has been reported in a variety of areas, including storm prediction and research, air quality modeling, wildfire, hurricane, tropical storm prediction, and regional climate and weather prediction (Michalakes et al., 2004). In this study, WRF is used for the downscaling of weather and climate at the scales from one kilometer to thousands of kilometers, and it is used for deriving meteorological parameters required for hydrological models. The model uses a terrain-following hydrostatic pressure coordinate system with permitted vertical grid stretching (Laprise, 1992). Arakawa-C grid staggering is used for horizontal discretization. The model equations are conservative for scalar variables. A detailed description of WRF is presented in Skamarock et al. (2008). For this study, two-way nested computational domains of 40×54×27 and 100×120×27 grid points and horizontal resolutions of 25 km and 5 km, respectively, were established. The first domain covers most of the Gansu Province, China ranging from 32.6° to 47.4°N in latitude and 92.4°–107.6°E in longitude. The second domain covers the Heihe River Basin, ranging from 37° to 43°N in latitude and 96.6°–103.4°E in longitude (Fig. 1). The model is initialized by real boundary conditions using NCAR-NCEP's Final Analysis (FNL) data (NCEP-DSS083.2, 2009), with a resolution of 1° × 1° (111 km × 111 km). A ratio of 1:5 is maintained between the resolutions of the outer domain and FNL data to ensure reliable boundary conditions for the model. The WRF simulations were carried out on a Dell R900, Ubuntu 9.10, g95 compiler with gcc.

2.2   Study area

This research was carried out in the Heihe River Basin, China's second largest inland river basin. The basin is located between 97°24′–102°10′ E and 37°41′–42°42′ N and covers an area of approximately 140000 km². The landscapes here are diverse, with an upstream to downstream distribution of glacier, frozen soil, alpine meadow, forest, irrigated crops, riparian ecosystem, desert, and gobi.

2.3   Data

Long-term of temperature from 2000 to 2009 has been simulated in WRF model. The model was tested at 15 surface meteorological stations maintained by the CMA and seven observation-strengthened stations established by WATER. The data from the CMA stations were used for daily validation and those of WATER for hourly validation. All data in 2008 were used for comparison. Table 1 lists the
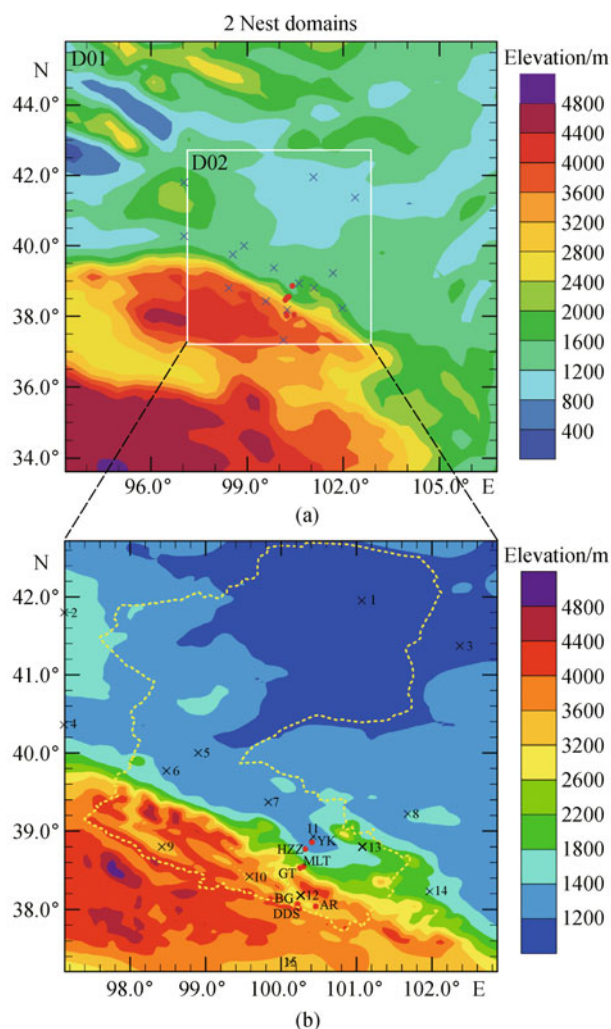
Fig. 1 Nesting domain configuration for the numerical experiment (the crosses indicate CMA stations, the red dots indicate WATER stations)

geographical and annual mean surface air temperatures at these stations.

3   Results

3.1   Spatial-temporal temperature characteristic of the Heihe River Basin

Figure 2 is the spatial distribution map of the average 2 m temperature simulated by WRF model from 2003 to 2009 in the Heihe River Basin. The average of 2 m temperature from 2003 to 2009 for whole Heihe River Basin is around 277.9 K. Figures 3 (a1–a7) show the difference of the average 2 m temperature of every year from that of total years and Fig. 3b demonstrates the 2 m temperature change trend from 2003 to 2009. Despite there are fluctuations in the trend line, but the overall trend is upward, the annual growth is around 0.1 K.

3.2   WRF output daily validation

Figure 4 shows the relationship of the daily surface air temperatures between the WRF model simulation and the observed data from the 15 surface meteorological stations maintained by CMA. As is evident, the simulated and observed surface temperatures show a significantly similar trend, with a correlation more than 0.93.

Table 2 lists the mean bias error, the root-mean-square error and the coefficient of determination between the WRF-simulated and observed data. The absolute mean bias error (MBE) for each station is less than 2°C, and the MBEs of Ejina, Mazongshan and Alax are near zero, which can be taken as unbiased estimations. For all stations, the RMSEs are approximately 2°C.

3.3   WRF output hourly validation

Hourly observation data are available from the seven sites supported by the WATER Project for 2008. Figure 5 shows the relationship of the hourly surface air temperatures between the WRF model simulation and the observation data from the seven observation-strengthened stations of WATER. Figure 6 compares the WRF simulation with bilinear interpolation and observation data from the Arou station in August. The original data for bilinear interpolation are temperatures extracted from the first domain of the WRF model at a 25 km resolution and were interpolated to a 5 km resolution. The MBE, RMSE and R^2 between the observed and simulation data can be found in Table 3.

3.4   Comparison with GCM reanalysis

Reanalysis data are long-term and stable collections of gridded atmospheric data, and are generated by a unified data assimilation system for quality control and data fusion, with the input data for this system including ground-based observations, ship observations, balloon observations, radiosonde wind observations, aircraft observations, satellite observations and other information (Kalnay et al., 1996; Kistler et al., 2001; Uppla et al., 2005; Onogi et al., 2007). Reanalysis data from JRA-25, ERA-40 and NCEP-II were selected for the validation of the WRF simulation. The features of JRA-25, ERA-40 and NCEP-II are listed in Table 4. The Fortran program was used to extract point temperature data from these reanalysis for each station. All reanalysis temperature data are transformed by topographic correction.

Figure 7 shows the comparison of MBE of the surface air temperature between the observed and three analyses and WRF simulations in the Heihe River Basin at the 15 stations. Obviously, the MBE of the WRF simulation is less than the three reanalysis data, especially at the Ejina and Mazongshan stations. The comparison at all stations indicates that the dynamic downscaling data are more reliable than the reanalysis data. Figure 7 compares the

Table 1   Geographic and annual mean surface air temperatures at the validation stations

Station type	Station name	Station ID	Altitude/m	Latitude/°N	Longitude/°E	Ta/°C
CMA	Ejina*	52267	940.5	41.57	101.04	9.99
	Mazongshan*	52323	1770.1	41.48	97.02	5.23
	Guaizihu	52378	960.0	41.22	102.22	10.13
	Yumenzhen	52436	1526.0	40.16	97.02	7.71
	Jinta	52447	1270.2	40.00	98.54	8.94
	Jiuquan*	52533	1477.2	39.46	98.29	7.90
	Gaotai	52546	1332.2	39.22	99.50	8.03
	Alax	52576	1510.1	39.13	101.41	9.01
	Tuole	52633	3367.0	38.48	98.25	−1.94
	Yeniugou	52645	3320.0	38.25	99.35	−2.47
	Zhangye	52652	1482.7	38.56	100.26	8.34
	Qilian	52657	2787.4	38.11	100.15	1.75
	Shandan	52661	1764.6	38.48	101.05	7.03
	Yongchang	52674	1976.1	38.14	101.58	5.82
	Menyuan	52675	2850.0	37.23	101.37	1.73
WATER	Arou	AR	3032.8	38.04	100.46	−0.95
	Binggou	BG	3449.0	38.07	100.22	Apr−Dec
	Dadongshu	DDS	4146.8	38.01	100.24	−5.44
	Guantan	GT	2835.2	38.53	100.25	Exclude Apr
	Huazhaizi	HZZ	1726.0	38.46	100.25	Jun−Dec
	Maliantan	MLT	2817.0	38.55	100.30	Jan−Jun Nov−Dec
	Yingkelvzhou	YK	1519.1	38.86	100.41	Exclude May Exclude Jul−Sep

Note: Stations marked with "*" are part of the WMO data that are already assimilated in the NCEP model
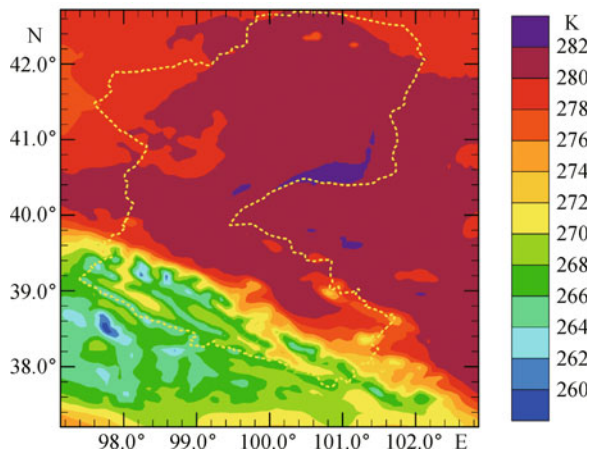
Fig. 2   Spatial distribution map of 2 m temperature from 2003 to 2009

differences among the WRF simulation, NCEP reanalysis, JRA reanalysis and station data, indicating that the WRF simulation is more astringent than the others. Compared with the bilinear interpolation result from the NCEP reanalysis (Fig. 7), WRF simulated data are closer to the

station observed data. Figure 8 shows the relationship between the Arou observed data and the WRF simulation, NCEP reanalysis and JRA reanalysis data in August. The NCEP and JRA reanalysis data were downscaled by elevation with a fixed temperature lapse rate (0.65°C/100 m) from coarser resolution to a 5 km resolution to match the resolution of the WRF output data.

4   Discussion

Downscaling is a method for obtaining high-resolution climate or climate change information from relatively coarse-resolution GCMs. Statistical downscaling derives statistical relationships between observed small-scale (often station level) variables and larger (GCM) scale variables, and is used more frequently than dynamical downscaling for surface temperature applications, such as analog methods (Ngo-Duc et al., 2005), regression analysis (Winkler, et al., 1997; Wilby et al., 1999; Hanssen-Bauer et al., 2005), and neural network methods (Mpelasoka et al., 2001). However, dynamical downscaling has a clearer physical description than statistical downscaling. In our
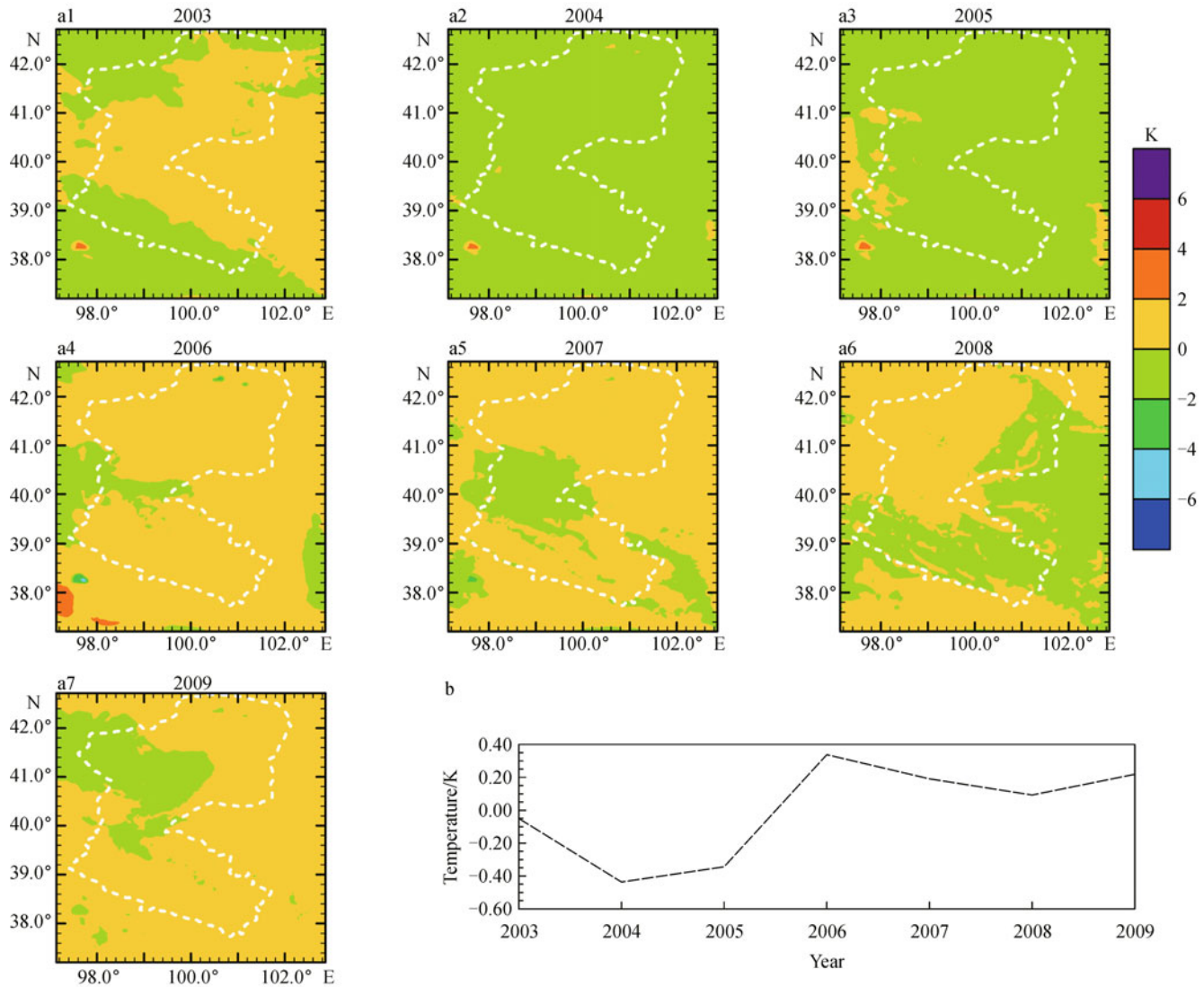
Fig. 3   Difference of the average 2 m temperature of every year from that of total years

research, the near-surface air temperature data by dynamic downscaling agreed well with our daily and hourly observed data.

Figures 6–8 show that the WRF simulation is better than the reanalysis data or interpolation results. The comparisons of daily (Fig. 7) and hourly (Fig. 4, four times per day: 00, 06, 12, 18) temperatures between the reanalysis and WRF simulations show that the WRF simulation is better than the reanalysis simulations. The WRF simulation (in Fig. 6) also yields better surface air temperature data than those interpolated from the FNL data (FNL is an initial for the WRF model).

WRF also has the ability of data assimilating of observation data and remote sensing images in the OBSGRID and WRF-Var modes under the support of the WATER Project, producing rich observation data. With our own data and remote sensing images in the WRF

simulation, the accuracy of surface temperatures will be greatly improved.

5   Conclusions

In this study, the WRF model was used to generate 5 km/1 h atmospheric forcing data for a hydrological scale model of the Heihe River Basin. The WRF results were validated by daily-observed data from CMA stations and hourly-observed data from WATER sites. The daily validation shows that the WRF simulation has good agreement with the observed data. The R^2 between the WRF simulation and each station is more than 0.93, the absolute MBE for every station is less than 2°C, and the MBEs of Ejina, Mazongshan and Alxa are near zero with an R^2 above 0.98, which can be taken as an unbiased estimation. The MBE of
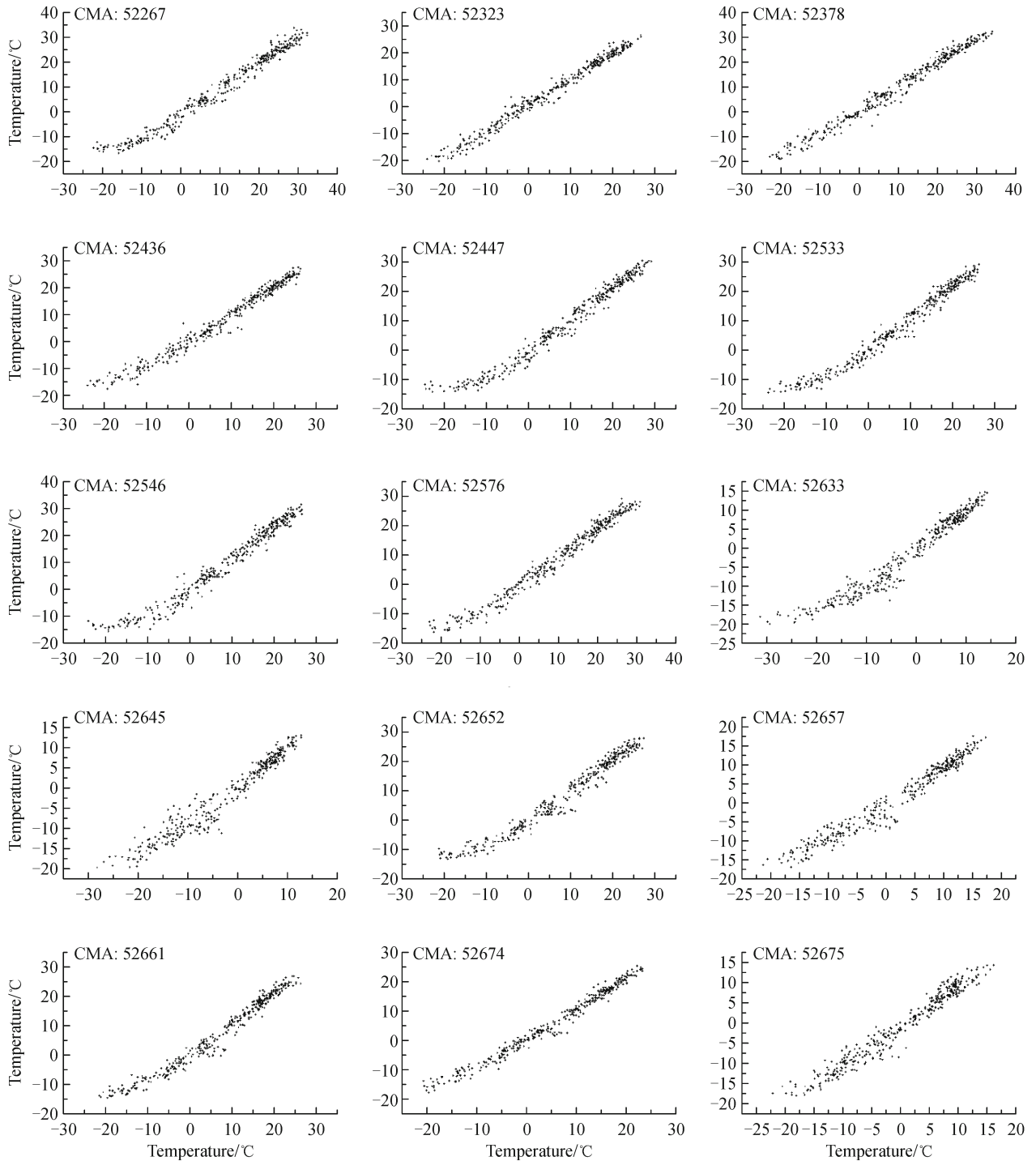
Fig. 4 Scatter plots of daily surface air temperature between the WRF simulation and station observation

every site is approximately 2°C, and the R^2 of every site is more than 0.80, with the highest at 0.95, while the computed and observed surface temperatures show a significantly similar trend. The comparison between the simulated and observed surface air temperatures shows

that the WRF succeeds in generating the meteorological inputs required for hydrological simulation. The results indicate that the dynamic downscaling air temperature fields have good correlations with observed daily and hourly data, and they are more reliable than the reanalysis

Table 2 MBE, RMSE and R^2 between the WRF simulated daily surface air temperature and 15 CMA stations data

Station name	Station ID	MBE/°C	RMSE/°C	R^2	95% confidence interval
Ejina	52267	0.21	2.15	0.98	(−0.02, 0.44)
Mazongshan	52323	0.00	1.88	0.98	(−0.20, 0.20)
Guaizihu	52378	−0.67	2.13	0.98	(−0.90, −0.45)
Yumenzhen	52436	−1.31	2.54	0.98	(−1.58, −1.04)
Jinta	52447	−0.90	2.53	0.98	(−1.16, −0.64)
Jiuquan	52533	−1.15	2.12	0.98	(−1.37, −0.93)
Gaotai	52546	−0.78	1.99	0.98	(−1.00, −0.57)
Alax	52576	−0.16	2.11	0.98	(−0.38, 0.06)
Tuole	52633	1.57	2.04	0.96	(1.36, 1.78)
Yeniugou	52645	1.77	2.49	0.94	(1.51, 2.03)
Zhangye	52652	−0.77	1.82	0.98	(−0.96, −0.58)
Qilian	52657	0.91	2.01	0.97	(0.70, 1.12)
Shandan	52661	1.27	1.74	0.98	(1.09, 1.45)
Yongchang	52674	1.12	1.82	0.98	(0.93, 1.31)
Menyuan	52675	1.76	2.30	0.94	(1.52, 2.00)

Notes: MBE: mean bias error; RMSE: root-mean-square error; R^2: coefficient of determination
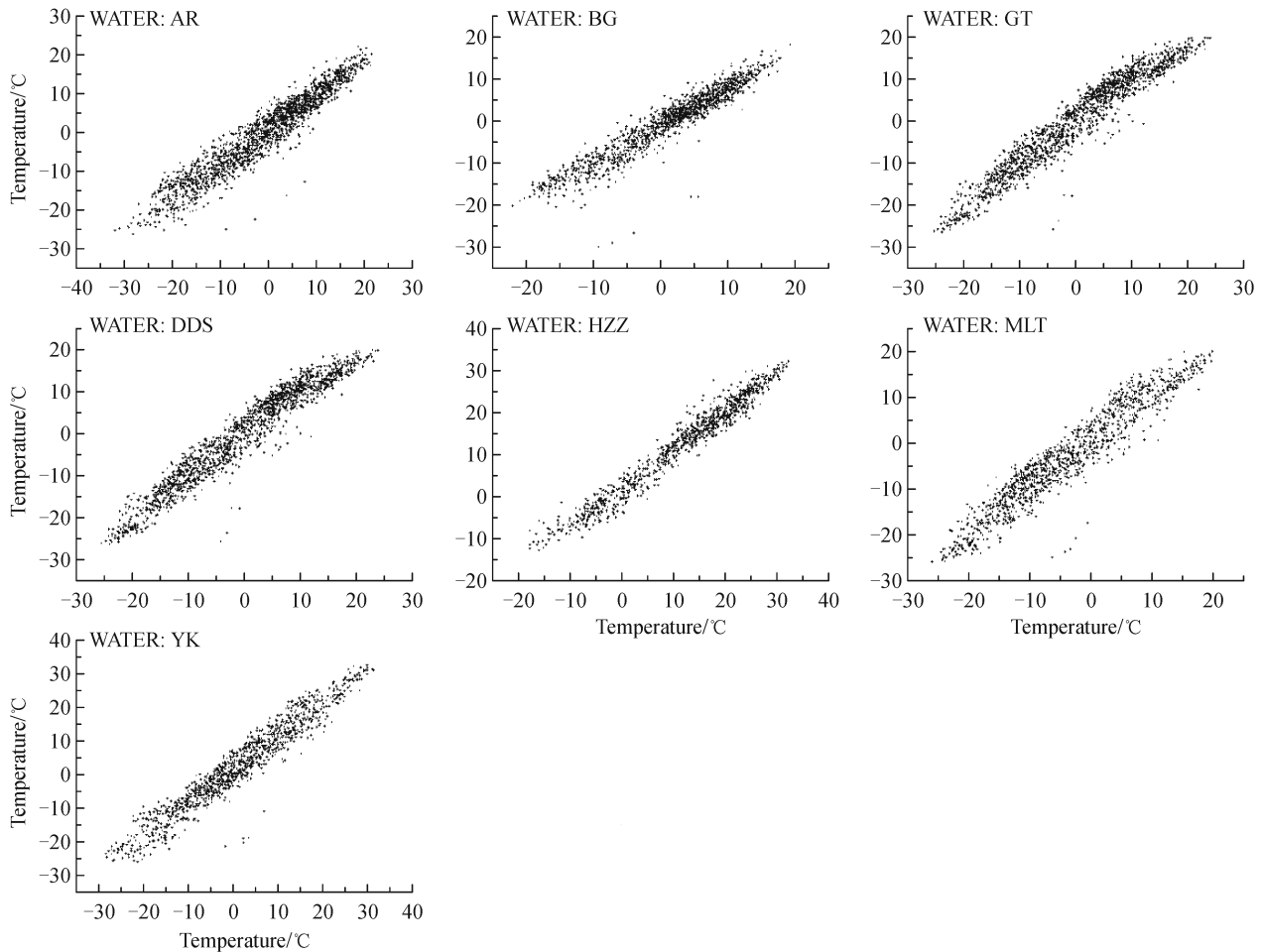
Fig. 5 Scatter plots of hourly surface air temperature between the WRF simulation and WATER observation
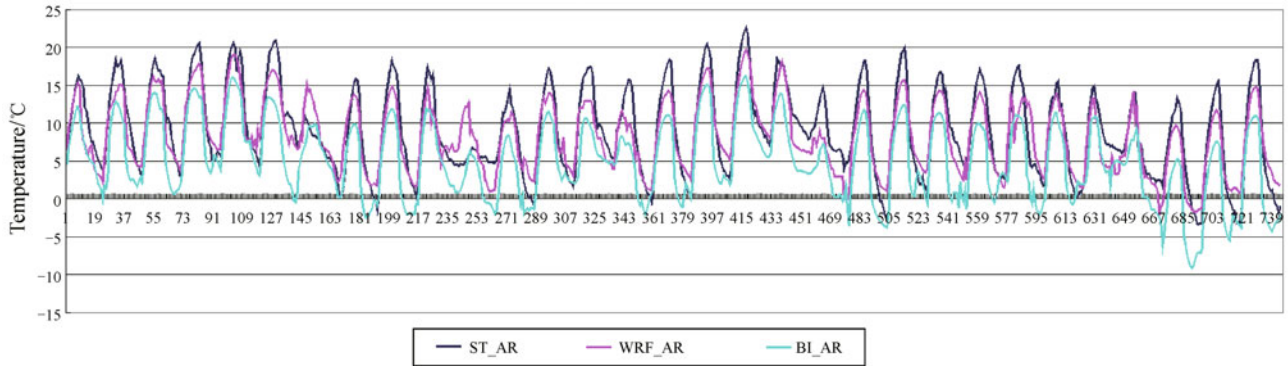
Fig. 6 Comparison of hourly surface air temperatures among the WRF-simulated, bilinear interpolation and observed data for the Arou station

Table 3 MBE, RMSE and R^2 between the WRF simulated hourly surface air temperature and seven WATER in-situ data

Station ID	MBE/°C	RMSE/°C	R^2	95% confidence interval
AR	0.35	2.87	0.92	(0.29, 0.41)
BG	−1.46	2.69	0.93	(−1.52, −1.40)
DDS	−1.19	2.21	0.94	(−1.24, −1.14)
GT	−0.66	1.71	0.94	(−0.70, −0.62)
HZZ	0.70	2.48	0.94	(0.65, 0.75)
MLT	0.70	3.09	0.92	(0.63, 0.77)
YK	1.30	3.16	0.94	(1.23, 1.37)

Table 4 Features of JRA-25, ERA-40 and NCEP-II

Name	Organization	Reanalysis period	Resolution	Data assimilation method
JRA-25	JMA/CRIEPI	1979 – present	T106 L40	3D-Var
ERA-40	ECMWF	Sep 1957 – Aug 2002	TL159 L60	3D-Var
NCEP-II	NCEP/DOE	1979 – present	T62 L28	3D-Var

Notes: T and TL indicate the wave transition numbers; L indicates the number of vertical levels; T106 and TL159 are equivalent to a grid interval of 120 km, and T62 is 200 km
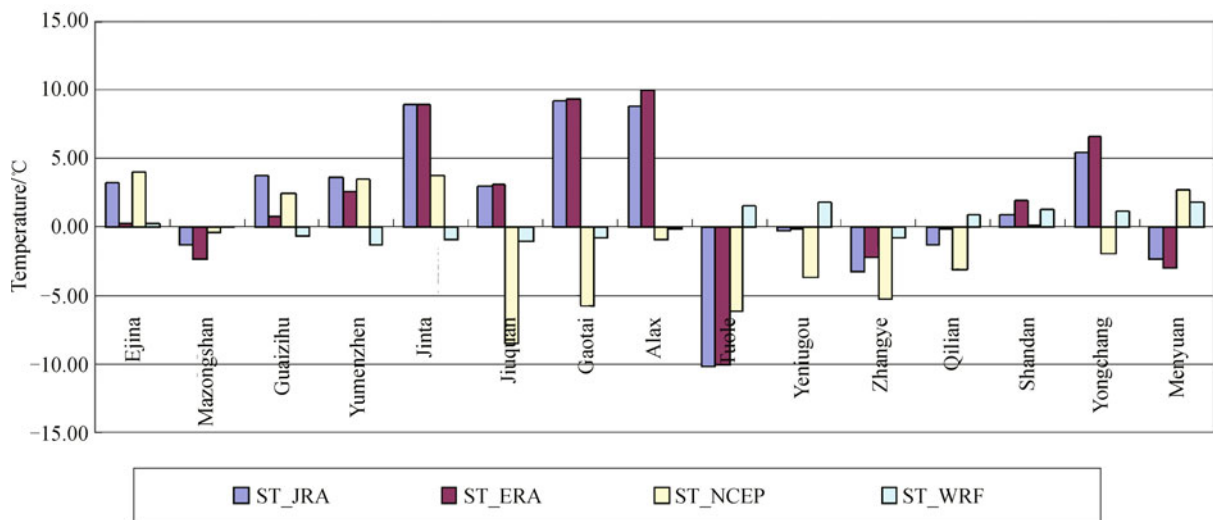
Fig. 7 Comparison of the MBE of the surface air temperatures between the observed and three reanalysis and WRF simulations in the Heihe River Basin (JRA-25, ERA-40 and NCEP-II: monthly MBE for ten years (1991–2000), WRF simulation: daily MBE for 2008)
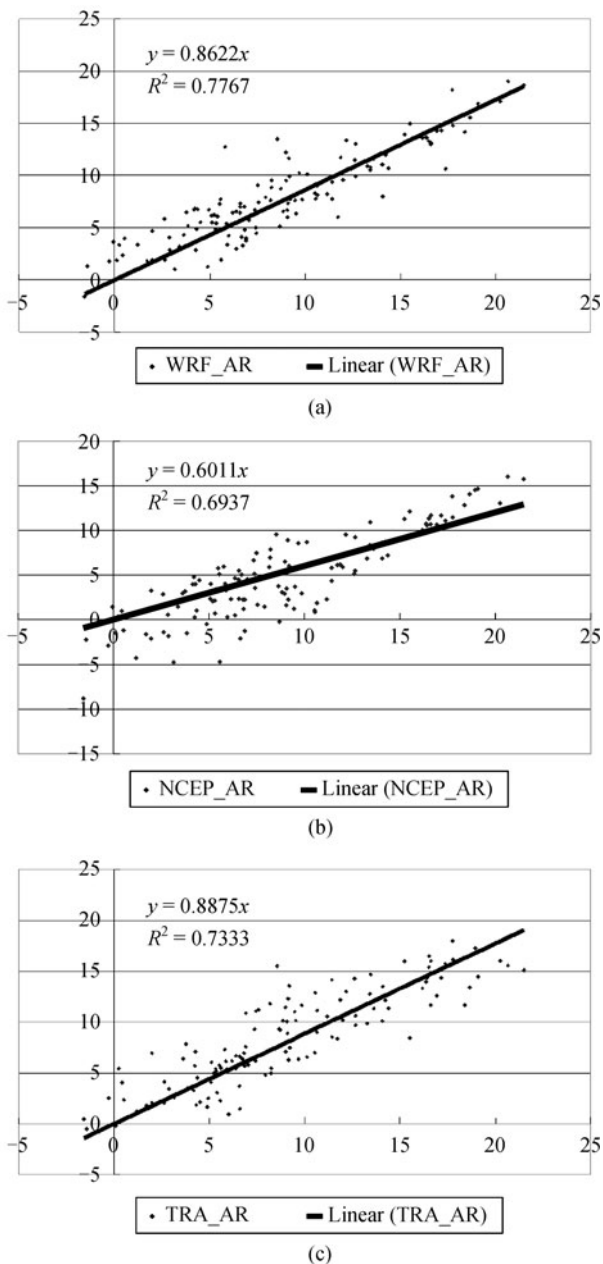
Fig. 8 Comparison of the relationship between (a) WRF simulation, (b) NCEP reanalysis, and (c) JRA reanalysis data for the Arou station in August

data. The WRF model is effective for downscaling air temperature.

References

Chen D, Achberger C, Räisänen J, Hellström C (2006). Using statistical downscaling to quantify the GCM-related uncertainty in regional climate change scenarios: a case study of Swedish precipitation. Adv Atmos Sci, 23(1): 54–60

Collischonn W, Haas R, Andreolli I, Tucci C E M (2005). Forecasting River Uruguay flow using rainfall forecasts from a regional weather-prediction model. J Hydrol (Amst), 305(1–4): 87–98

Cosgrove B A, Lohmann D, Mitchell K E, Houser P R, Wood E F, Schaake J C, Robock A, Marshall C, Sheffield J, Duan Q, Luo L, Higgins R W, Pinker R T, Tarpley J D, Meng J (2003). Real-time and retrospective forcing in the North American Land Data Assimilation System (NLDAS) Project. J Geophys Res, 108(D22): 1–12

Hanssen-Bauer I, Achberger C, Benestad R E, Chen D, Førland E J (2005). Statistical downscaling of climate scenarios over Scandinavia. Clim Res, 29(3): 255–268

Jasper K, Gurtz J, Lang H (2002). Advanced flood forecasting in Alpine watersheds by coupling meteorological observations and forecasts with a distributed hydrological model. J Hydrol (Amst), 267(1–2): 40–52

Kalnay E, Kanamitsu M, Kistler R, Collins W, Deaven D, Gandin L, Iredell M, Saha S, White G, Woollen J, Zhu Y, Leetmaa A, Reynolds R, Chelliah M, Ebisuzaki W, Higgins W, Janowiak J, Mo K C, Ropelewski C, Wang J, Jenne R, Joseph D (1996). The NCEP/NCAR 40-year reanalysis project. Bull Am Meteorol Soc, 77(3): 437–471

Kislter R, Kalnay E, Collins W, Saha S, White G, Woollen J, Chelliah M, Ebisuzaki W, Kanamitsu M, Kousky V, Dool H, Jenne R, Fiorino M (2001). The NCEP/NCAR 50-year reanalysis: monthly means CD-ROM and documentation. Bull Am Meteorol Soc, 82(2): 247–267

Kunstmann H, Jung G, Wagner S, Clottey H (2008). Integration of atmospheric sciences and hydrology for the development of decision support systems in sustainable water management. Phys Chem Earth, 33(1–3): 165–174

Kunstmann H, Stadler C (2005). High resolution distributed atmospheric-hydrologic modeling for Alpine catchments. J Hydrol (Amst), 314(1–4): 105–124

Laprise R (1992). The Euler equation of motion with hydrostatic pressure as independent coordinate. Mon Weather Rev, 120(1): 197–207

Leander R T, Buishand A (2007). Resampling of regional climate model output for the simulation of extreme river flows. J Hydrol (Amst), 332 (3–4): 487–496

Leander R, Buishand T A, van den Hurk B J J M, de Wit M J M (2008). Estimated changes in flood quantiles of the river Meuse from resampling of regional climate model output. J Hydrol (Amst), 351 (3–4): 331–343

Li X, Li X W, Li Z Y, Ma M, Wang J, Xiao Q, Liu Q, Che T, Chen E, Yan G, Hu Z, Zhang L, Chu R, Su P, Liu Q, Liu S, Wang J, Niu Z, Chen Y, Jin R, Wang W, Ran Y, Xin X, Ren H (2009). Watershed allied telemetry experimental research. J Geophys Res, 114(D22103): 1–19

Lu G, Wu Z, Wen L, Zhang J (2006). Application of a coupled

atmospheric-hydrological modeling system to real-time flood forecast. Advances in Water Science, 17(6): 847–852 (in Chinese)

Michalakes J, Chen S, Dudhia J, Hart L, Klemp J, Middlecoff J, Skamarock W (2001). Development of a Next Generation Regional Weather Research and Forecast Model in developments in teracomputing. In: Zwieflhofer W, Kreitz N, eds, Proceedings of the 9th ECMWF Workshop on the Use of High Performance Computing in Meteorology. Singapore: World Scientific, 269–276

Michalakes J, Dudhia J, Gill D, Klemp J, Shamarock W (1998). Design of a next-generation regional weather research and forecast model: towards teracomputing, World Scientific, River Edge, New Jersey, 117–124

Michalakes J, Dudhia J, Gill D, Henderson T, Skamarock W, Wang W (2004). The weather reseach and forecast model: software architecture and performance. In: Proceedings of the 11th ECMWF Workshop on the Use of High Performance Computing in Meteorology, 25–29 October, 2004.

Mpelasoka F S, Mullah A B, Heerdegen R G (2001). New Zealand climate change information derived by multivariate statistical and artificial neural networks approaches. Int J Climatol, 21(11): 1415–1433

Ngo-Duc T, Polcher J, Laval K (2005). A 53-year forcing data set for land surface models. J Geophys Res, 110(D06116): 13

Onogi K, Tsutsui J, Koide H, Sakamoto M, Kobayashi S, Hatsushika H, Matsumoto T, Yamazaki N, Kamahori H, Takahashi K, Kadokura S, Wada K, Kato K, Oyama R, Ose T, Mannoji N, Taira R (2007). The JRA-25 reanalysis. J Meteorol Soc Jpn, 85(3): 369–432

Skamarock W C, Klemp J B, Dudhia J, Gill D O, Barker D M, Duda M G, Huang X Y, Wang W, Power J G (2008). A description of the advanced research WRF Version 3. www.mmm.ucar.edu/ wrf/users/ docs/user_guide/ARWUsersGuide.pdf (accessed June 2008)

Uppla S M, KÅllberg P W, Simmons A J, Andrae U, Bechtold V D C, Fiorino M, Gibson J K, Haseler J, Hernandez A, Kelly G A, Li X, Onogi K, Saarinen S, Sokka N, Allan R P, Andersson E, Arpe K, Balmaseda M A, Beljaars A C M, Berg L V D, Bidlot J, Bormann N,

Caires S, Chevallier F, Dethof A, Dragosavac M, Fisher M, Fuentes M, Hagemann S, Hólm E, Hoskins B J, Isaksen L, Janssen P A E M, Jenne R, Mcnally A P, Mahfouf J F, Morcrette J J, Rayner N A, Saunders R W, Simon P, Sterl A, Trenberth K E, Untch A, Vasiljevic D, Viterbo P, Woollen J (2005). The ERA-40 reanalysis. Q J R Meteorol Soc, 131(612): 2961–3012

Wilby R L, Hay L E, Gutowski W J Jr, Arritt R W, Takle E S, Pan Z, Leavesley G H, Clark M P (2000). Hydrological responses to dynamically and statistically downscaled climate model output. Geophys Res Lett, 27(8): 1199–1202

Wilby R L, Hay L E, Leavesley G H (1999). A comparison of downscaled and raw GCM output: implications for climate change scenarios in the San Juan River Basin, Colorado. Journal of Hydro1ogy, 225 (1–2): 67–91

Winkler J A, Palutikof J P, Andresen J A, Goodess C M (1997). The simulation of daily temperature time series from GCM output: Part II: Sensitivity analysis of an empirical transfer function methodology. J Clim, 10(10): 2514–2532

Yu Z, Barron E J, Yarnal B, Lakhtakia M N, White R A, Pollard D, Miller D A (2002). Evaluation of basin-scale hydrologic response to a multi-storm simulation. J Hydrol (Amst), 257(1–4): 212–225

Xiaoduo Pan was born in 1978. She received the B. S. and M. S. in physical geography from the Lanzhou University, China, in 2000 and 2003, respectively, and received M. A. in international environment from the Tokyo University of Agriculture and Technology University, Japan. Now, she is a Ph.D. candidate of the Cold and Arid Regions Environmental and Engineering Research Institute, Chinese Academy of Sciences. Her current research interests focus on atmospheric forcing data for land surface model and downscale method.